O$_2$ photoabsorption in the 40 950–41 300 cm^{-1} region: New Herzberg bands, new absorption lines, and improved spectroscopic data

T. G. Slanger, D. L. Huestis, and P. C. Cosby
Molecular Physics Laboratory, SRI International, Menlo Park, California 94025

H. Naus[a)] and G. Meijer
Department of Molecular and Laser Physics, University of Nijmegen, Toernooiveld 1, 6525 ED Nijmegen, The Netherlands

The technique of cavity ring-down (CRD) spectroscopy is particularly useful for measuring absorptions of very weak optical transitions. We have in this manner investigated the 40 950–41 300 cm^{-1} region in O$_2$, where only absorption in the O$_2(A\ ^3\Sigma_u^+ - X\ ^3\Sigma_g^-)$ 11-0 band had been previously identified. Five new bands have been discovered in this range—the $A'\ ^3\Delta_u - X\ ^3\Sigma_g^-$ 12-0 and 13-0 bands, the $c\ ^1\Sigma_u^- - X\ ^3\Sigma_g^-$ 17-0 and 18-0 bands, and the $A\ ^3\Sigma_u^+ - X\ ^3\Sigma_g^-$ 12-0 band. The origins of the F_1 and F_2 components of the latter lie only 7 cm^{-1} below the lowest dissociation limit, and 15 lines have been identified. No F_3 levels were observed; apparently all are above the dissociation limit. The high instrumental sensitivity of the CRD technique has allowed observation of weak lines of the $A-X$ 11-0 band, and 12 of the 13 branches have been identified and their intensities measured. A very low upper limit has been set on the intensity of the thirteenth branch, Q_{13}. We find 107 unidentified lines in the region, the stronger ones (19) lying in the vicinity of lines of the $A-X$ 11-0 band. The weaker ones (88) are spread throughout the spectral region, up to and even beyond the O$_2$ dissociation limit, and probably have their origin in transitions to very weakly bound O$_2$ states, which may have atmospheric significance. These weaker lines have intensities that are typically 1%–5% of the strong $A-X$ 11-0 band lines. © *1996 American Institute of Physics.* [S0021-9606(96)01545-0]

INTRODUCTION

The ultraviolet terrestrial nightglow is dominated by emission from electronically excited oxygen.[1] The emitters are the three so-called Herzberg states, which are generated by the recombination of oxygen atoms.[2] These in turn are produced by daytime O$_2$ photodissociation in the Schumann–Runge bands and continuum at 130–205 nm.

The most detailed laboratory spectroscopic studies of the Herzberg transitions* were carried out by Borrell *et al.*,[3] Coquart and Ramsay,[4] and Ramsay.[5] The nomenclature for the Herzberg systems is as follows: Herzberg I $A\ ^3\Sigma_u^+ - X\ ^3\Sigma_g^-$; Herzberg II $c\ ^1\Sigma_u^- - X\ ^3\Sigma_g^-$; Herzberg III $A'\ ^3\Delta_u - X\ ^3\Sigma_g^-$. The highest vibrational levels that they reported were $v=11$ for the $A\ ^3\Sigma_u^+$ state ($\nu_0=41\ 153.92$ cm^{-1}),[3] $v=11$ for the $A'\ ^3\Delta_u(\Omega=1)$ state ($\nu_0=40\ 988.15$ cm^{-1}),[4] and $v=16$ for the $c\ ^1\Sigma_u^-$ state ($\nu_0=40\ 860.62$ cm^{-1}).[5] As the O$_2\ ^3P_2 + ^3P_2$ dissociation limit lies at 41 267.5 cm^{-1},[6] there is room for at least one more vibrational level in the A' state, and at least two in the c state. In the A' state, the energy spacing between the last two observed levels, $v=10$ and 11, is 301 cm^{-1},[4] while in the c state, the spacing between $v=15$ and 16 is 212 cm^{-1}.[5] As for the A state, it has not been clear from a Birge–Sponer plot that the next level, $v=12$, would be stable.

We have recently presented the results of a cavity ring-down (CRD) study of O$_2$ photoabsorption in the 243–250 nm region, undertaken for the purpose of making band strength measurements on the Herzberg transitions.[7] In the course of this investigation, we observed lines above 40 950 cm^{-1} that were not associated with the $A-X$ 11-0 band, the only one listed by Ramsay and colleagues[3–5] in this region. In fact, we have found numerous uncataloged lines, some of which are associated with the three Herzberg states, and others with an as-yet-unidentified O$_2$ transition. In this report we identify the new $A(v=12)$, $A'(v=12,13)$, and $c(v=17,18)$ levels, identify branches and measure intensities for the $A-X$ 11-0 band that do not appear in recent tabulations,[3,8] and present a list of 107 lines which remain to be identified.

INTRODUCTION TO CRD SPECTROSCOPY

In 1988 O'Keefe and Deacon[9] introduced cavity ring-down (CRD) spectroscopy as a sensitive technique to perform direct absorption measurements using pulsed light sources. The CRD technique is based on a measurement of the rate of absorption rather than the magnitude of absorption of a light pulse confined in an optical cavity with a high Q factor. The method has the advantages of direct absorption spectroscopic techniques, but avoids the sensitivity problems due to light source intensity fluctuations, while a stable optical cavity design allows for highly effective multipassing.

O'Keefe and Deacon demonstrated in their first experiments[9] that the sensitivity of the method in the visible region of the spectrum is superior to the sensitivity of conventional absorption spectroscopy. Since then it has been shown that the technique can be used to perform sensitive

---

[a)]Present address: Dept. of Physics and Astronomy, Laser Centre, Free University of Amsterdam, 1081 HV Amsterdam, The Netherlands.

absorption spectroscopy in a molecular jet expansion,[10,11] and we have recently used it to measure the beam intensity in a laser-desorption jet-cooling mass spectrometer.[12] Romanini and Lehmann[13] have used CRD for a spectroscopic study of the stretching overtones in HCN. In the latter experiments, mirrors with a reflectivity $R = 0.9999$ were used and a noise-equivalent absorption coefficient in the 10^{-10} cm^{-1} region was reported.

Yu and Lin[14] have shown that CRD can be used for quantitative kinetics measurements as well, and recently, Scherer *et al.*[15] have performed CRD experiments in the infrared region of the spectrum. We have shown that CRD spectroscopy can be performed with high spectral resolution and good sensitivity even in relatively short cavities. We have applied the technique for the first time to the uv part of the spectrum, as far as 200 nm,[16,17] and have applied it for trace gas detection in various environments.[18] Around 250 nm, where mirrors with a reflectivity better than 0.997 are not yet available, absorption down to 10^{-7} cm^{-1} is still readily detected.[7]

THEORY OF CRD SPECTROSCOPY

If a monochromatic light pulse at frequency ν is coupled into an otherwise empty cavity, the ring-down transient $I_{CRD}(t)$ is a single exponentially decaying function of time with a $1/e$ ''cavity ring-down time'' $\tau(\nu)$ which is solely determined by the reflectivity $R(\nu)$ of the mirrors and the optical pathlength d between them. The presence of absorbing species in the ring-down cavity can now be deduced from the resulting decrease in the cavity ring-down time. It follows, therefore, that in the more general case $I_{CRD}(t)$ is proportional to

$$I_{CRD}(t) \propto \int_0^\infty I(\nu) e^{-t/\tau(\nu)} \, d\nu, \tag{1}$$

where $\tau(\nu)$ is given by

$$\tau(\nu) = \frac{d}{c(|\ln(R(\nu))| + \Sigma_i \sigma_i(\nu) \int_0^d N_i(x)dx)}, \tag{2}$$

where c is the velocity of light, and the sum is over all light scattering and absorbing species with frequency dependent cross sections $\sigma_i(\nu)$ and a line-integrated number density $\int_0^d N_i(x)dx$.[9,13,18]

As long as the laser linewidth is spectrally narrower than the absorption feature of the species under study, the time dependence of the light intensity inside the cavity is correctly described with a single exponentially decaying curve.[18,19] We reiterate that in a CRD experiment the *rate* of absorption of a light pulse confined in a closed optical cavity is measured, and the measurement is therefore independent of light source intensity fluctuations, as long as the spectral intensity distribution of the light stays constant from pulse to pulse.

EXPERIMENT

For the experiments described in this paper, a stable optical cavity formed by placing two identical 25 mm diameter

planoconcave mirrors with a radius of curvature of -25 cm at 45.5 cm distance, is used. The mirrors are coated for optimum reflectivity at 248 nm ($R = 0.996$ at 248 nm). All the measurements have been performed with either 500 mBar or 1000 mBar of pure molecular oxygen in the ring-down cavity. The higher pressure is used only in the high frequency region of the spectrum, where the oxygen absorption lines are already somewhat broader. We note, however, that due both to the increase in linewidths of the molecular absorption (pressure broadening) and the overall reduction in the cavity ring-down time as a consequence of Rayleigh scattering, the detection sensitivity only improves slightly by doubling the pressure.

The required laser radiation in the 243–250 nm range is produced by pumping a dye laser operating with Coumarin 480 dye with the third harmonic of a Nd:YAG laser at 355 nm (Spectra Physics GCR-150, PDL-3 combination). The output of the dye laser is frequency doubled in a BBO crystal, typically producing 1 mJ of laser radiation with a bandwidth of 0.2 cm^{-1}. For the experiments described in this paper, about 1 μJ of tunable radiation in a 2 mm diameter spot is directed along the 45.5 cm long cavity, and only a small fraction of this (on the order of 10^{-3}) is coupled into the cavity through the highly reflecting mirror. Mode matching of the laser beam with the ring-down cavity is omitted so as to set up a near-continuum of modes inside the cavity.[16]

The time dependence of the light intensity in the stable optical cavity is monitored via detection of the light that leaks out through the other mirror, using a photomultiplier placed in close proximity. The PMT signal is amplified and fed into a digitizing oscilloscope with ten bit vertical resolution and 10 ns sampling time (LeCroy 9430). Typically, 25 ring-down transients, all taken at the same laser frequency, are added in the 16-bit memory of the oscilloscope, and the sum is subsequently read out by a 486-PC.

To be able to accurately determine the baseline of the cavity ring-down transients, approximately 100 data points are recorded and averaged prior to the start of the ring-down transient. This averaged baseline is subtracted from those data points of the ring-down transient that are recorded within a pre-set time interval from the start of the transient, a time-interval which is typically chosen as three $1/e$ decay times of the empty cavity. Subsequently, the natural logarithm of the data is taken and fit to a straight line using a weighted least-squares fitting algorithm.[20] It is the slope of this fitted line which is recorded as a function of the laser frequency.

The time-constant that describes the decay of the empty cavity in our set-up is around 250 ns, and its exact value can be determined to an accuracy of approximately 10^{-3}. The laser is stepped over the desired spectral range in 0.03 cm^{-1} increments (in the uv).

A small fraction of the fundamental wavelength of the dye laser is sent through a tellurium oven (heated to 450 C) for absolute wavelength calibration.[21] The Te$_2$ absorption spectrum is recorded simultaneously with the O$_2$ CRD spectrum, and is used for calibration and linearization of the frequency scale. Comparison of the observed O$_2$ absorptions to

the precisely known $A-X$ 11-0 line positions[3,8] suggests that lines are measured in the present work with an accuracy of ± 0.1 cm^{-1}.

With this frequency scale, the individual line positions are then determined with a line-fitting program (QUASIL) developed at SRI. Linewidths are obtained from isolated lines, and these widths are then used in subsequent analysis of weaker or merged features.

RESULTS AND DISCUSSION

Our earlier paper[7] described the application of CRD spectroscopy to forbidden transitions in O$_2$. The virtue of the technique is its very high sensitivity to absorption features, and we took advantage of this capability to measure line strengths in the three Herzberg systems.

The laser linewidth used in the earlier measurements was on the order of 0.5 cm^{-1}, which resulted in some problems in dealing with strong Herzberg I lines, as they have a Doppler width of only ~ 0.08 cm^{-1}. For this reason, we stressed that under those conditions, the measurements on the weaker Herzberg II and III systems were more reliable. Nevertheless, our evaluation and recommendations for the $A-X$ oscillator strengths are in excellent agreement with more recent measurements of Yoshino *et al.*[22]

The laser linewidth has now been reduced to ~ 0.20 cm^{-1}, both for the purpose of improving line position data, and to obtain more realistic line strengths. The main point of the present work is to use the intrinsic sensitivity of the CRD system to investigate energy levels near the O$_2$ dissociation limit which have not previously been observed by other techniques. The narrower linewidth is advantageous in searching for very weak lines, as it helps to differentiate them from the background.

New Herzberg I, II, III spectra

The DIATOM spectral simulation program was described in the earlier study.[7] We have used it to calculate line positions in the five new bands, based on extrapolations of the existing spectroscopic data for the lower vibrational levels.[3,8]

Trial values of the band origins and rotational constants were estimated by extrapolation from the lower levels to the dissociation limit. A mass-scaled interpolation/extrapolation was also used to provide predictions for our comparison study of ^{18}O$_2$. For all three Herzberg states, we found that plots of v (the vibrational quantum number) against $(D_0-E)^{1/2}$ were nearly linear, where D_0 is the energy of the dissociation limit,[6] 41 267.5 cm^{-1}, and E is the vibrational term energy, or G_v, with all energies measured relative to the (nonexistent) $J=N=0$ F_2 level of the ground state. This allowed us to determine the number of bound vibrational levels to be expected and to estimate the energies of the previously unobserved ones. For the rotational constant, B_v, extrapolation comes from a plot of $[(D_0-E)/(D_0-G_0)]^n$ vs B_v. The exponent n was chosen to give a smooth graph that is approximately linear as $D\rightarrow D_0$ and $B_v\rightarrow 0$. The values for n chosen for the three states lie in the range 0.1–0.3. In these calculations, we make the assumption that the three

states dissociate to the lowest atomic limits, $^3P_2+^3P_2$. This limit is consistent with an adiabatic correlation of the A, A', and c states to the separated atoms.[23] The next limit lies 158 cm^{-1} higher, and we have no evidence that the higher limits become involved.

Once the data and the DIATOM simulation are in reasonable agreement, the individual line positions are assigned, and a nonlinear least-squares fit is made to determine the effective constants of the Hamiltonian describing the upper state.[24]

Figure 1 shows portions of the spectra, the $\Omega=2$ head of the $A'-X$ 12-0 band (1a), near the head of the $c-X$ 17-0 band (1b), and the head of the $A-X$ 12-0 band (1c). In each case, comparison is made with the DIATOM simulations, although there may be discrepancies of tenths of cm^{-1} between the DIATOM output and the final fit. This is not surprising, as different Hamiltonians are used. Tables I–V list the lines in the five bands, along with the differences obtained from the best fit. The constants used in these fits are given in Table VI. As may be seen, some of the parameters were frozen when insufficient data were available for a complete analysis.

From these fits, rotational term energies are calculated for the five new levels, using the ground state energies of Amiot and Verges.[25] The upper state term energies are displayed graphically in Fig. 2, plotted against $J(J+1)$. Also included in the plot are the known $A(v=11)$ and $A'(v=11)$ levels.[3,4] In none of the five new levels do we find shifts attributable to perturbations, although we do not preclude energy shifts less than 0.1 cm^{-1}. Inspection of Fig. 2 shows that there are no crossings of A $^3\Sigma_u^+$ and c $^1\Sigma_u^-$ levels, the only combination that might lead to perturbations. Yoshino *et al.*[8] have reported detecting perturbations in the $v=12$ and 15 levels of the O$_2(c)$ state, caused by crossings with the $v=7$ and 9 levels of the A state, respectively.

The $A(12)$ level lies very near to the dissociation limit, and parameterizing its levels in terms of meaningful molecular constants is particularly difficult, especially in view of the fact that only four rotational levels ($N=1,3,5,7$) are observed in the F_2 substate and only three levels ($N=1,3,5$) are observed in the higher energy F_1 substate. No $v=12$ levels are observed for the F_3 substate, which by analogy with the lower vibrational levels, should lie yet higher in energy, most probably in the dissociation continuum.

The band origin and rotational constant B for $A(12)$ listed in Table VI have been derived solely from the F_2 levels. A centrifugal distortion constant was not required to fit the four levels. That is, D was held fixed at zero. However, a rather large value for D is calculated[26] for $v'=12$ from the *ab initio* potential energy curve of the A state,[27] $D=1.2\times10^{-4}$ cm^{-1}. In Table VI, the upper entry gives the molecular constants obtained from the fit to the observed lines using $D=0$, while the lower entry gives those constants obtained using $D=1.2\times10^{-4}$ cm^{-1}.

The fine-structure splitting constants for $A(12)$ also can be only poorly determined from the observed levels. The values list in Table VI are rough extrapolations from the lower vibrational levels. An accurate determination of the
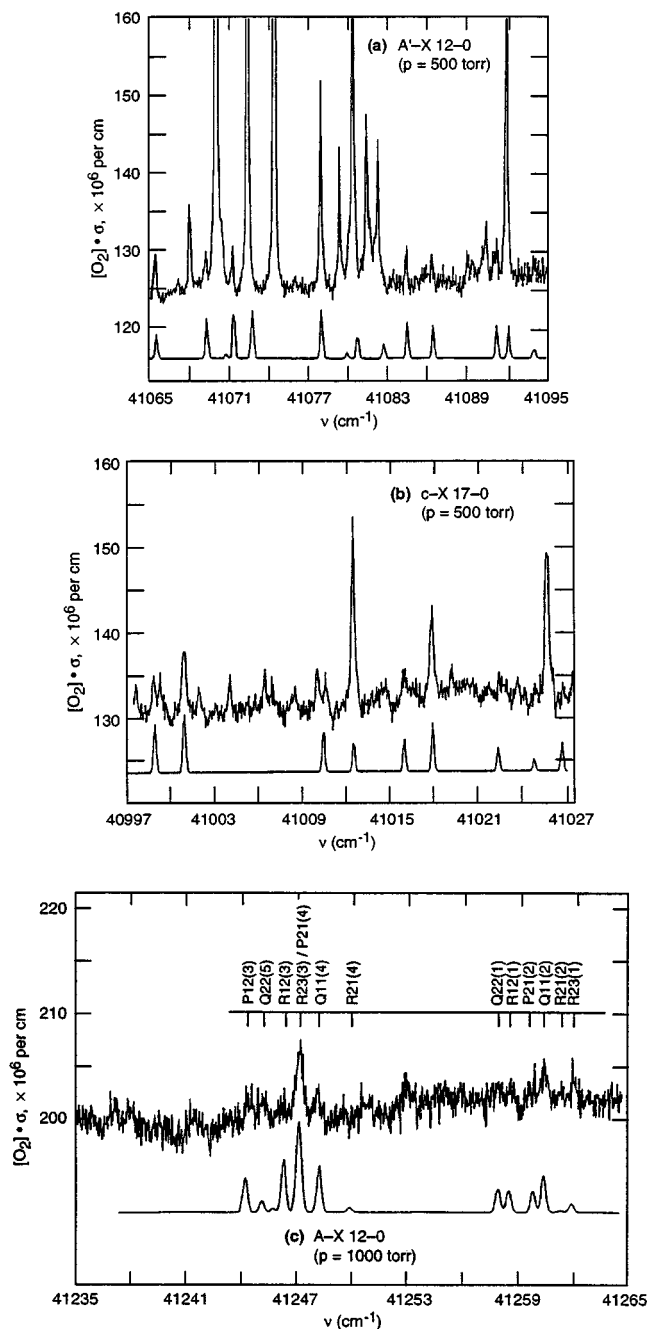
FIG. 1. CRD spectra, plus simulations. (a) The $\Omega=2$ head of $A'-X$ 12-0; the strongest lines belong to the $A-X$ 11-0 band. (b) Near the head of $c-X$ 17-0. (c) The head of $A-X$ 12-0.

TABLE I. $A\ ^3\Sigma_u^+ - X\ ^3\Sigma_g^-$ 12-0 line positions (cm^{-1}).

N''	Branch	Observed line position	Obs−Calc	Average upper state term energy
1	Q_{11}	41 260.45	+0.00	41 261.54
3		41 248.15	−0.22	41 263.50
5		41 226.03	+0.00	41 267.29
1	Q_{22}	41 257.91	−0.03	41 260.83
3		41 245.18	−0.11	41 262.42
1	R_{12}	41 258.60	+0.03	41 261.54
3		41 246.26	−0.16	41 263.50
5		41 224.26	+0.22	41 267.29
1	P_{21}	41 259.78	−0.04	41 260.78
1	R_{23}	41 262.02	+0.12	41 260.83
3	P_{21}/R_{23}	41 247.18	−0.10/+0.04	41 262.42
5		41 224.26	+0.01/+0.03	41 265.39
7		41 191.20	−0.12/+0.08	41 269.70[a]
3	P_{12}	41 244.43	+0.24	41 261.54
5		41 220.42	−0.12	41 263.50
7		41 186.81	+0.14	41 267.29

[a]The feature at the $P_{21}/R_{23}(7)$ line position is stronger than expected, and may not be that line. It is the only $A(12)$ line with an upper state term energy that appears to exceed the nominal O₂ dissociation energy of 41 267.5 cm^{-1}. The three entries in the P_{21}/R_{23} branch with multiple obs−calc are from duplicate measurements.

similar values, with $F_3(N)$ approximately -2λ higher

$$F_1(N)\approx F_2(N)+(2N+2)B+\gamma(N+1)$$
$$+(2N+3)^2 B^2/(2\lambda), \tag{3}$$
$$F_3(N)\approx F_2(N)-2\lambda-(2N-2)B-\gamma N$$
$$-(2N-1)^2 B^2/(2\lambda). \tag{4}$$

In the limit of large negative λ, $F_1(N)$ is only weakly dependent on the value of λ chosen. Assuming $\lambda=-15$ cm^{-1}, the final term in the energy expression has a calculated value of only -0.15 cm^{-1} for $N=5$, the highest level observed.

The value of the constant λ can be varied within the approximate range of -5 cm$^{-1}>\lambda>-20$ cm^{-1} and still reproduce the spacings of the observed F_1 and F_2 levels to

TABLE II. $c\ ^1\Sigma_u^- - X\ ^3\Sigma_g^-$ 17-0 line positions (cm^{-1}).

N''	Branch	Observed line position	Obs−Calc
1	^RQ	41 026.30	+0.03
3		41 017.53	−0.06
5		41 000.54	+0.01
7		40 975.08	+0.02
9		40 941.08	−0.01
1	^PP	41 022.02	+0.04
3		41 010.20[a]	+0.18
5		40 989.76	+0.00
7		40 961.14	−0.03
3	^RR	41 015.66	+0.02
5		40 998.50	−0.04
7		40 973.10	+0.06
9		40 939.03	+0.02
5	^PQ	40 991.72	−0.05
7		40 963.14	+0.00

[a]Line not used in fit to obtain molecular constants.

spin-rotation constant, γ, would not be expected given that only very low rotational quantum numbers and two spin components are observed in the present work. The spin–spin constant, λ, is more interesting. Based on the values from the lower vibrational levels, we expect λ to be large and negative. When combined with the fact that the rotational constant for $A(12)$ is very small, this means that Hund's case (c) is appropriate. The F_1 and F_2 components are almost pure combinations of $\Omega=\pm1$, while the F_3 component is predominantly $\Omega=0$. The term energies $F_1(N)$ and $F_2(N)$ have

TABLE III. $c\ {}^1\Sigma_u^- - X\ {}^3\Sigma_g^-$ 18-0 line positions (cm^{-1}).

N''	Branch	Observed line position	Obs−Calc
1	${}^R Q$	41 150.53	+0.04
5		41 122.01	−0.10
1	${}^P P$	41 146.70	+0.03
3		41 134.42^a	+0.19
5		41 112.78	−0.09
7		41 043.16	−0.09
1	${}^R R$	41 148.40^a	−0.21
5		41 120.05	+0.13
13		40 954.06	+0.00
3	${}^P Q$	41 136.28	−0.04
5		41 114.80	−0.08
9		41 045.15	−0.04
11		40 996.84	+0.02

^{a}Line not used in fit to obtain molecular constants.

within their experimental accuracy. A value for λ within this range would be consistent with a vibrational extrapolation of this constant from the lower levels of the A state, but such an extrapolation relies heavily on the perturbed $A(11)$ level.

The magnitude of λ in the A state is, to first order, determined by the off-diagonal spin–orbit coupling between the $A\ {}^3\Sigma_u^+$ state and the $c\ {}^1\Sigma_u^-$ and $B\ {}^3\Sigma_u^-$ states, which have its same $\pi^3\pi^{*3}$ electronic configuration.[27] *Ab initio* values for these matrix elements have been calculated by Klotz and Peyerimhoff[29] for internuclear distances in the range of 2.3 to 2.9 a.u. The coupling with the B state is sufficiently small that its effect on λ is negligible. Given the *ab initio* potential energy curves for the A and c states,[27] and presuming a linear extrapolation of the spin–orbit matrix element as a function of internuclear distance, the value of lambda as a function of vibrational level can be calculated from[29]

$$\lambda_v = \frac{1}{2} \sum_{v'} \frac{A(r_{vv'})^2 \langle v|v'\rangle^2}{E_v^A - E_{v'}^c},\qquad (5)$$

where $A(r_{vv'})$ is the spin–orbit matrix element evaluated at the R centroid for the pair of A state and c state vibrational levels, $\langle v|v'\rangle$ is the vibrational overlap integral, the denominator is the difference in energy between the vibrational levels, and the summation extends over all vibrational levels of the $c\ {}^1\Sigma_u^-$ state.

The values of λ_v calculated from Eq. (5) agree with experimental observations to within 11% for $v\leqslant 9$. However, the calculated values for $v=10,11,12$ are $\lambda = -6.56,\ -12.1,$ and -38.6 cm^{-1}, respectively, which are only qualitatively in accord with the experimental values for $v=10$ and 11 ($\lambda = -5.846$ and -7.79 cm^{-1})[5] and the present estimated range for the value of λ_{12} (-15 cm^{-1} in Table VI). Because these higher vibrational levels probe an increasingly large range of internuclear separations, the representation of the A state by a single electronic configuration should become increasingly less appropriate. Thus a confident estimate of λ_{12} either from an empirical extrapolation or a simple calculation is not possible. Hence, the values of λ and γ given for $A(12)$ in Table VI represent only those values used to generate the simulated spectra.

TABLE IV. $A'\ {}^3\Delta_u - X\ {}^3\Sigma_g^-$ 12-0 line positions (cm^{-1}). (A) $\Omega=1$ sub-bands. (B) $\Omega=2$ subbands. (C) $\Omega=3$ subbands.

(A) N''	Branch	Observed line position	Obs−Calc
1	R_{33}	41 199.14	+0.03
3		41 187.70^b	+0.01
5		41 170.40^b	−0.01
9		41 122.86^b	−0.01
3	Q_{33}	41 184.81	+0.02
5		41 165.60	+0.01
7		41 138.75	−0.02
11		41 062.05	+0.00
5	P_{33}	41 161.75	+0.01
9		41 096.58	−0.02
5	R_{32}	41 174.15	−0.02
7		41 151.16	−0.03
1	R_{31}	41 201.87	+0.02
3		41 196.21	−0.01
5		41 182.85	−0.02
1	Q_{31}	41 198.98	+0.02
3		41 191.41	+0.00
5		41 176.13	−0.02
9		41 122.51	+0.01
5	P_{31}	41 170.37^b	−0.01
9		41 112.95^b	−0.02

(B) N''	Branch	Observed line position	Obs−Calc
3	R_{22}	41 084.40	−0.08
5		41 069.17	+0.01
7		41 046.23	+0.08
11		40 976.78	−0.07
5	Q_{22}	41 184.81	−0.10
7		41 165.60	+0.00
9		41 138.75	+0.15
11		41 062.05	+0.06
1	R_{21}	41 096.88	−0.01
3		41 091.30	+0.07
5		41 077.85^b	−0.01
7		41 056.75	+0.00
9		41 027.91	+0.04
13		40 946.63	+0.02
1	Q_{21}	41 094.00	+0.00
3		41 086.31^a	−0.12
5		41 071.12	−0.03
7		41 048.22	+0.06
11		40 978.85	−0.06
5	P_{21}	41 065.36^b	−0.04
7		41 040.50^b	−0.03
9		41 008.03^{a,b}	+0.11
11		40 967.62^b	+0.06

(C) N''	Branch	Observed line position	Obs−Calc
3	R_{12}	40 977.07^a	+0.23
5		40 961.51	+0.01
5	Q_{12}	40 955.75	−0.01

^{a}Lines not used to obtain molecular constants.
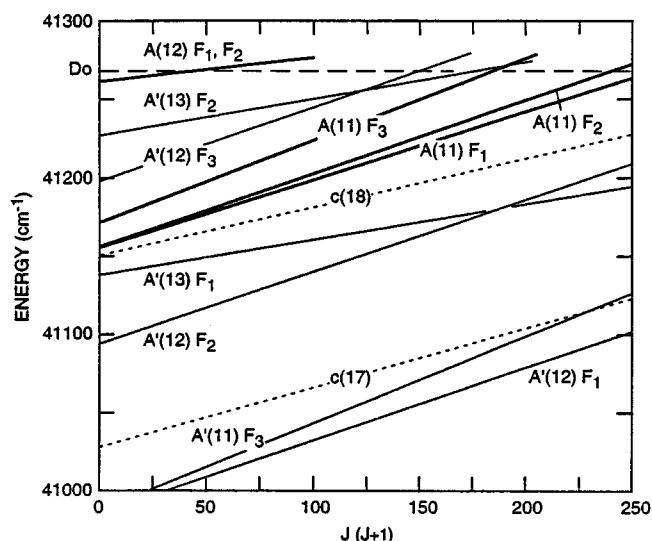$^b P_{31}/R_{33}$ and P_{21}/R_{23} are blended for $N''>1$.

Transitions into all three spin-orbit components of the $A'(12)$ level are observed in the present work. Following the earlier determination[30] of the molecular constants for the lower levels of the A' state, both the γ and λ constants were

TABLE V. A' $^3\Delta_u$–X $^3\Sigma_g^-$ 13-0 line positions (cm^{-1}). Ω=2 subbands.

N''	Branch	Observed line position	Obs−Calc
3	R_{23}	41 213.06[a]	−0.01
7		41 161.64[a]	−0.20
3	Q_{23}	41 211.44	+0.00
5		41 189.36	+0.10
7		41 157.69	+0.05
9		41 116.20	−0.16
1	R_{22}	41 223.63	−0.10
3		41 213.06	−0.07
5		41 193.03	+0.02
7		41 163.29	+0.02
9		41 123.66	+0.09
3	Q_{22}	41 210.96	−0.02
5		41 190.15[b]	+0.25
7		41 159.20	−0.05
9		41 118.82	+0.01
9	P_{22}	41 114.14[b]	−0.27
13		41 001.66	−0.15
3	R_{21}	41 217.66	−0.07
5		41 198.76	+0.15
7		41 169.95[b]	+0.26
9		41 130.59	−0.08
3	Q_{21}	41 215.22	+0.14
7		41 165.56[b]	+0.28
9		41 125.60	−0.01
11		41 075.86	+0.18
3	P_{21}	41 213.06[a]	+0.13
7		41 161.64[a]	+0.24

[a]P_{21}/R_{23} are blended for $N''>1$.
[b]Line not used in fit to obtain molecular constants.

included, together with the effective spin–orbit coupling constant A, in the $^3\Delta$ Hamiltonian to describe the $A'(12)$ levels. The fit yields very large values for both $\gamma(1.27\pm0.06$ cm$^{-1})$ and $\lambda(-0.53\pm0.03$ cm$^{-1})$. While such values are not inconsistent with the values determined in the lower vibra-

FIG. 2. Upper state term energies vs $J'(J'+1)$ for levels at 41 000–41 300 cm^{-1}.

tional levels, they must be viewed as being unphysically large relative to the value $\lambda=0$ which has been estimated for this state from theory.[27] A better representation of the $A'(^3\Delta_u)$ levels is achieved by constraining γ to a value $\gamma=0$, and fitting the constants A, A_D, and λ, where A_D is the centrifugal distortion contribution to the diagonal spin–orbit splitting constant A. The results of this fit for $A'(12)$ are given in Table VI. It should be noted that this choice of constants is able to fit all observed levels[4] of the $A'(11)$ state to within their experimental accuracies, whereas the previous choice of constants for the Hamiltonian could not.

Only transitions into a single spin-orbit component, F_2 ($\Omega=2$), of the $A'(13)$ level are observed in the present work.

TABLE VI. O$_2$ Molecular constants for the new Herzberg levels. Band origins are referenced in energy to O$_2$ X $^3\Sigma_g^-$ ($N=J=0$). All units are cm^{-1}.

Constant	$A(12)$	$A'(12)$	$A'(13)$	$c(17)$	$c(18)$
ν_0	41 270.480(88)[a]	41 092.815(42)	41 225.339(150)	41 024.854(46)	41 149.546(74)
	41 270.449(97)[c]				
$\nu_0(F_2)$[b]	41260.490	41 094.019	41 226.080		
	41260.471[c]				
B	0.1626(42)	0.4826(11)	0.2741(48)	0.4030(19)	0.3232(24)
	0.1684(46)[c]				
$D(10^5)$	0.0[f][d]	3.32(51)	18.2(29)	6.4(17)	4.2(11)
	12.0[f][c]				
λ	−15.0[f]	−0.197(26)	−0.15[f]		
$\gamma(10^3)$	−10.0[f]	0[f]	0[f]		
A		−52.193(26)	−39.0[f]		
$A_D(10^3)$		1.90(49)	1.0[f]		
# lines	19	49	23	16	11
Std dev	0.121	0.035	0.113	0.035	0.074
	0.141[c]				

[a]Number in parentheses represents two standard deviations expressed in units of the least-significant digits.
[b]Band origin describing the F_2 levels alone.
[c]Constants for $A(12)$ obtained with D constrained to the value calculated from the potential energy curve.
[d]Constant was frozen to this value.

Consequently, all spin-splitting constants were constrained to extrapolated values in the fits. These constrained values are listed in Table VI, together with the fitted rotational constants.

For consistency with other work and to facilitate a comparison of term values, all of the band origins in Table VI have been corrected to reference them to the (nonexistent) $N=J=0$ level of the O$_2$ X $^3\Sigma_g^-$ $(v=0)$ ground state. In addition, the origins (ν_0) of $c(17)$ and $c(18)$, and those origins labeled $\nu_0(F_2)$ for $A(12)$, $A'(12)$, and $A'(13)$ reference the upper state rotational levels relative to $J'(J'+1)-\Omega^2=0$, where $\Omega=0$ for the F_2 levels of $A(12)$ and $\Omega=2$ for the F_2 level in the A' state.

From the extrapolations described above, it is clear that the $v=19$ level of O$_2(c)$ is stable, lying some 40 cm^{-1} below the dissociation limit. Although there are numerous candidate lines in the region, we have not been able to convincingly demonstrate its presence. With a narrower laser linewidth, it should be discernible. The ν_{00} value is expected to be close to 41 228 cm^{-1}, and the rotational constant should be 0.20–0.23 cm^{-1}. This band origin puts it very close to the new $A'(v=13)$ level. The calculations suggest that $v=20$ should also be stable, lying 3 cm^{-1} below the dissociation limit, i.e., very close to $A(v=12)$. Again, improved experiments will be needed to identify the last O$_2(c)$ level.

Line intensities in the $A-X$ 11-0 band

Yoshino *et al.*[8] have recently made new absorption measurements on the O$_2(A-X)$ system, using a Fourier transform spectrometer operating in the uv. For the 11-0 band, they reported line positions in only 8 of the 13 branches. In a subsequent paper,[22] the intensity of a single line in the $^OP_{23}$ branch was reported, as was a blended line in the $^SR_{21}$ branch. A correction to be noted is that assignments are made for the $Q_{33}(N=1)$ line in several of the bands; such a line does not exist.

The greater sensitivity of the CRD spectrometer has resulted in position and intensity data for 12 branches; only the $^OQ_{13}$ branch was not discernible, although an upper limit can be set that makes it more than an order of magnitude weaker than the next weakest branch. In Table VII we complete the $A-X$ 11-0 position listings, making comparisons to calculated positions derived from the term energies of Yoshino *et al.*[8] and of Amiot and Verges[25] for the O$_2$ ground state; agreement is quite satisfactory. Also listed are Herzberg's positions[31] for three of the five branches not listed by Yoshino *et al.*[8]

We note that Herzberg listed line positions in the Q_{13} branch for the $A-X$ 10-0 band.[31] These assignments seem to be incorrect; at least two of the five lines can be attributed to the $A'-X$ 11-0 band, and in any case the Q_{13} lines are expected to be too weak to measure.

Considerable effort has been spent since Herzberg's original publication[32] in attempting to quantify and rationalize the intensities of the $A-X$ rotational branches.[32–34] The recent work of Huestis *et al.*,[7] Yoshino *et al.*,[22] and England

TABLE VII. Line positions and intensities for $A-X$ 11-0 band (cm^{-1}+40 000). First entry: calculation from term energies [Yoshino *et al.* (Ref. 8), Amiot and Verges (Ref. 25)]. Second entry: CRD data. Third entry: Herzberg (1952). Fourth entry: relative experimental intensities/[CRD data −calculation].

N''	R_{32}	P_{23}	Q_{31}	R_{21}
1	171.02		172.90	158.93
	170.92		172.81	Blended
	170.80		172.66	
	4.5/−0.10		8/−0.09	
3	164.39	139.85	166.34	153.62
	164.34	139.93	166.25	Blended
	164.34	139.90	166.17	
	6/−0.05	4/+0.08	12/−0.09	
5	150.63	118.82	152.62	140.19
	150.53	118.82	152.58	140.29
	150.49	118.34	152.62	
	3/−0.10	9/0.00	8/−0.04	3/+0.10
7		090.40	131.14	118.83
		090.50	Blended	118.82
		090.23		
		7/+0.10		9/−0.01
9		053.92	102.25	091.92
		053.90	102.30	Blended
		054.14		
		8/−0.02	12/+0.05	
11		009.54	064.99	054.93
		009.64	064.98	054.93
		009.59	064.71	
		5/+0.10	10/−0.01	5/0.00
13		959.63		
		959.55		
		959.82		
		5/−0.08		

et al.[35] has clarified the situation for $v'\leq 10$, and we are now in a position to provide additional information on the weak branches in $v'=11$.

For the 11-0 band, Yoshino *et al.*[22] have reported integrated intensities for the eight stronger branches. Since we know that the CRD spectra tend to underestimate the line strength, we make relative comparisons, where the measured intensities are summed and the branch intensities are expressed as a fraction of the total sum for each value of N. In Table VIII we list these relative intensities for the CRD data and the values of Yoshino *et al.*[22] In addition, we also present the values given by the DIATOM program. For the Q_{13} branch only an upper limit can be given from the CRD data, but it is in agreement with the analysis reported by England *et al.*[35] for the $A-X$ 10-0 band. For the same band, a Q_{13} value 200 times larger is listed by Cann and Nicholls.[34] As discussed by Huestis *et al.*,[7] the model of Cann and Nicholls for the $A-X$ rotational branch strengths is an empirical representation of the line intensities reported by Herzberg[31] for only two N values in the 10-0 band. It is now clear that Herzberg's Q_{13} lines are misidentifications. The model used in the DIATOM program was described by Huestis *et al.*[7] The spectral simulations reported here use the transition-strength parameters listed therein. The model used by England *et al.*[35] is equivalent, but with transition-strength parameters that have been changed slightly to optimize the fit with the ex-

TABLE VIII. Relative $A-X$ 11-0 line intensities.[a] Row 1—CRD spectra. Row 2—Yoshino *et al.* (Ref. 22). Row 3—DIATOM calculations.

N	Q_{11}	Q_{22}	Q_{33}	R_{12}	R_{23}/P_{21}	P_{32}	P_{12}	P_{23}	R_{21}	R_{32}	Q_{31}	Q_{13}	Σ
1	283	147		152	289	62				23	44		388
	266	168		188	264	114							447
	302	171		176	221	60			13	13	45		398
3	212	29	37	177	326	79	90	7		17	27	0.8	764
	190	52		198	377	98	85						839
	179	37	41	186	327	69	90	21	14	7	29	0.1	938
5	176	20	39	183	257	99	111		6	7	17		879
	222	26	36	208	323	102	83						1180
	171	25	33	192	343	87	89	19	16	3	22	1	1291
7	200	34	36	189	324	108	98	13					851
	182	34	44	196	347	115	74						851
	177	23	26	194	348	102	79	16	16	1	18	1	1471
9	200	26	40	165	342	116	67	17			29	0.3	892
	200	28	44	171	331	141	63	13	8				1177
	187	25	19	193	346	112	69	15	15	0.2	15	1	1486
11	193	28	43	158	322	122	75	21	12		29		763
	216	17	32	183	350	145	59						1032
	199	28	15	191	343	120	61	14	15	0.0	13	0.5	1369
13	197	31	27	153	380	164	44						637
	214	30	31	173	360	140	49						698
	221	34	11	195	353	130	57						1115

[a]For each N, the branch intensities sum to approximately 1000. Units in Σ column are 10^{-26} cm^2 cm^{-1}.

perimental line strengths reported subsequently by Yoshino *et al.*[22] The models are expected to be least reliable for $v'=11$ because it known to be strongly perturbed.

In the last column of Table VIII are presented the summed absolute integrated intensities for each N, in units of 10^{-26} cm^2 cm^{-1}. The DIATOM data originate with our recommended $A-X$ 11-0 oscillator strength.[7] It is clear that the CRD data have values 10%–30% smaller than the values of Yoshino *et al.*,[22] while the DIATOM calculations agree reasonably well with the latter, with an increasing discrepancy above $N=7$, i.e., as the dissociation limit is approached. Although there has been an improvement in the CRD data with narrowing of the laser linewidth, the problem with underestimation is still present, and is unlikely to be overcome without better matching of the absorption and laser linewidths, and an analytical treatment of the line shapes.

Inspection of Table VIII shows that the Q_{31} branch has an intensity comparable to that of Q_{22}, so it is surprising that the former was not reported by Yoshino *et al.* for any $A-X$ band.[8] These authors have displayed a spectrum for the $A-X$ 8-0 band, and in fact the $Q_{31}(N=5,7,9)$ lines are readily apparent, with an intensity comparable to the (reported) lines of the R_{21} branch, and about half that of Q_{22}. England *et al.*[35] and other authors[30,32,33] have listed Q_{31} line strengths.

Unidentified lines

After identifying as many of the new lines as possible, we are still left with a pool of more than 100 unidentified lines, listed in Table IX. These are divided between the 19 strong lines lying in the vicinity of $A-X$ 11-0 lines, previously noted by Borrell *et al.*[3] and Yoshino *et al.*,[8] but not tabulated by them, and the 88 weaker lines. The lines extend up to and even beyond the 41 267.5 cm^{-1} dissociation limit.

Yoshino *et al.*[8] have suggested that the strong lines are due to the very weakly bonded $^3\Pi_u$ state, which is certainly possible, and the same may be true for some of the weaker lines in Table IX. A glance at Fig. 2 demonstrates that the line shifts in the $A-X$ 11-0 band are unrelated to any of the new levels.

Borrell *et al.*[3] have measured and discussed these perturbations, finding line shifts as large as 1.5 cm^{-1}. Their favored explanation is that the perturber is the $^5\Sigma_u^-$ state, based on the potential curve calculations of Saxon and Liu.[36] From the data in Table I on the $v=12$ level, it is evident that there are no perturbations of a similar magnitude.

The lines listed in Table IX include the relative peak intensities, which are normalized to the absolute intensity of the $Q_{22}(7)$ $A-X$ (11-0) line, given by Yoshino *et al.*[22] as 47×10^{-26} cm^2 cm^{-1}. We are reasonably confident that these unidentified lines are associated with O$_2$, rather than with impurities. In the first place, they tend to die away near the 41 267.5 cm^{-1} dissociation limit, and more importantly, the 2 cm^{-1} ground state splitting between the F_1/F_3 and the F_2 components recurs often.
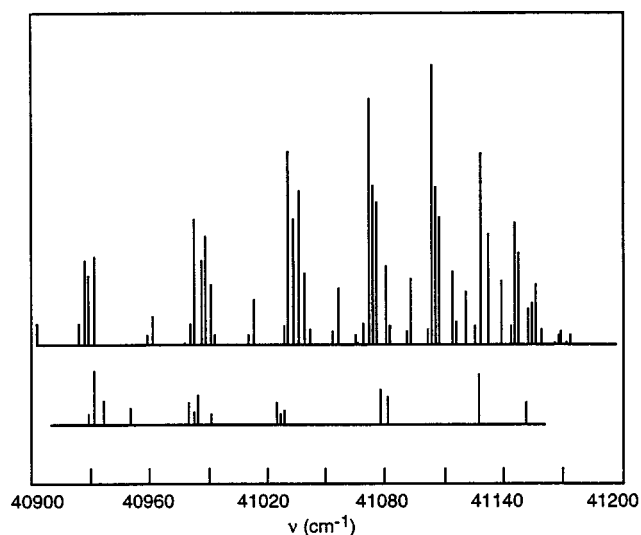
We show in Fig. 3 the relationship between the strong unidentified lines and the lines of the $A-X$ 11-0 band, demonstrating that indeed the latter occur in the vicinity of the former. On the other hand, the weak lines seem to be distributed throughout the spectral region, and show no obvious correlation either with the $A-X$ 11-0 band or bands in the other two Herzberg systems.

If the absorbing state is $^3\Pi_u$, the transition from the $^3\Sigma_g^-$ ground state would be fully allowed. The extreme weakness of the lines would then be associated with the Franck–Condon factors, which are minute, since the bound region of the $^3\Pi_u$ state is calculated to lie at very large interatomic

TABLE IX. (A) Catalog of unidentified lines associated with $A-X$ 11-0 band. (B) Catalog of other unidentified lines.

(A)	Frequency (ν) (cm^{-1})	Absorption cross section (σ) ($\times 10^{-26}$ cm^2 cm^{-1})
1	40 929.66	24
2	931.85	108
3	932.36	60
4	936.91	48
5	949.83	36
6	979.74	39
7	979.94	45
8	982.67	27
9	984.69	60
10	990.77	24
11	41 025.20	45
12	025.34	39
13	027.10	24
14	029.16	30
15	077.85	69
16	079.25	57
17	081.33	57
18	127.62	99
19	151.56	42

(B)	ν(cm^{-1})	σ($\times 10^{-26}$ cm^2 cm^{-1})		ν(cm^{-1})	σ($\times 10^{-26}$ cm^2 cm^{-1})
1	40 943.30	15	45	41 109.72	12
2	944.64	18	46	1 110.36	12
3	948.62	12	47	1 112.21	15
4	953.17	5	48	1 115.77	4.5
5	953.75	4.5	49	1 118.30	24
6	954.06	2.7	50	1 121.20	24
7	965.88	6	51	1 121.64	9
8	971.19	2.4	52	1 123.92	6
9	971.81	3.3	53	1 124.13	6
10	973.61	5	54	1 124.78	7.5
11	977.50	4.5	55	1 128.03	9
12	977.91	11	56	1 132.31	12
13	987.70	6.6	57	1 135.02	6
14	993.28	12	58	1 149.32	20
15	998.95	17	59	1 149.49	17
16	41 003.64	15	60	1 161.03	3.6
17	1 006.55	9	61	1 162.39	6.3
18	1 016.31	5.4	62	1 173.61	6
19	1 018.89	9	63	1 177.05	2.7
20	1 021.10	2	64	1 177.98	11
21	1 021.36	4	65	1 178.88	2.7
22	1 022.37	15	66	1 180.72	12
23	1 023.25	11	67	1 181.90	11
24	1 023.72	2.7	68	1 182.74	7.5
25	1 024.62	5.7	69	1 183.55	6.3
26	1 033.02	6.3	70	1 185.39	4
27	1 033.63	11	71	1 188.32	6
28	1 034.71	4.2	72	1 207.16	9
29	1 035.55	5	73	1 217.15	4
30	1 042.28	6	74	1 226.72	3
31	1 042.95	9	75	1 228.69	5.4
32	1 045.40	6	76	1 230.67	5
33	1 058.51	4	77	1 233.61	15
34	1 058.36	3.6	78	1 234.88	12
35	1 059.36	2.4	79	1 237.04	6
36	1 067.09	6	80	1 237.94	6
37	1 081.57	15	81	1 241.35	4.5
38	1 082.08	17	82	1 241.75	2.7
39	1 089.12	6	83	1 253.07	8
40	1 089.58	6	84	1 266.02	4
41	1 095.34	4.5	85	1 266.60	5
42	1 095.68	2.7	86	1 282.57	5
43	1 100.35	6.3	87	1 282.78	5
44	1 107.72	7.5	88	1 295.49	12

FIG. 3. $A-X$ 11-0 band (upper) and strong unidentified lines (lower).

spacings.[27] Hence, its transition strength must arise through its perturbation of the A state.

We are in the process of carrying out CRD measurements with ^{18,18}O$_2$, and hope that the new spectral information will help in the assignment of the unidentified lines. Early results indicate that the topmost $A\ ^3\Sigma_u^+$ level, $v=12$ in this isotopomer, is substantially perturbed.

CONCLUSIONS

The high sensitivity of CRD spectroscopy has led to a great improvement in O$_2$ spectroscopic information in the 40 950–41 300 cm^{-1} region. Five new bands have been found in the Herzberg systems $A-X$ 12-0, $A'-X$ 12-0, $A'-X$ 13-0, $c-X$ 17-0, and $c-X$ 18-0. The $A-X$ 12-0 band origin lies within 7 cm^{-1} of the molecular dissociation limit, and analysis will provide information on the O$_2$ long-range potential. More than 100 lines are still unidentified in the measured spectral region, and will probably lead to information on weakly bound O$_2$ states, as well as the last member of the $c-X$ system.

Absolute intensities are reported for the unidentified lines, and absolute and relative intensities for the $A-X$ 11-0 band, where information has been incomplete. The CRD study has led to identification of 12 out of the 13 branches of the band, with a low upper limit on the intensity of the thirteenth.

ACKNOWLEDGMENTS

[1] A. L. Broadfoot and K. R. Kendall, J. Geophys. Res. **73**, 426 (1968).

[2] T. G. Slanger, Science **202**, 751 (1978).

[3] D. A. Ramsay, Can. J. Phys. **64**, 717 (1986).

[4] B. Coquart and D. A. Ramsay, Can. J. Phys. **64**, 726 (1986).

[5] P. M. Borrell, P. Borrell, and D. A. Ramsay, Can. J. Phys. **64**, 721 (1986).

[6] P. C. Cosby and D. L. Huestis, J. Chem. Phys. **97**, 6108 (1992).

[7] D. L. Huestis, R. A. Copeland, K. Knutsen, T. G. Slanger, R. T. Jongma, M. G. H. Boogaarts, and G. Meijer, Can. J. Phys. **72**, 1109 (1994).

[8] K. Yoshino, J. E. Murray, J. R. Esmond, Y. Sun, W. H. Parkinson, A. P. Thorne, R. C. M. Learner, and G. Cox, Can. J. Phys. **72**, 1101 (1994).

[9] A. O'Keefe and D. A. G. Deacon, Rev. Sci. Instrum. **59**, 2544 (1988).

[10] J. J. Scherer, J. B. Paul, C. P. Collier, and R. J. Saykally, J. Chem. Phys. **102**, 5190 (1995).

[11] A. O'Keefe, J. J. Scherer, A. L. Cooksy, R. Sheeks, J. Heath, and R. J. Saykally, Chem. Phys. Lett. **172**, 214 (1990).

[12] M. G. H. Boogaarts and G. Meijer, J. Chem. Phys. **103**, 5269 (1995).

[13] D. Romanini and K. K. Lehmann, J. Chem. Phys. **99**, 6287 (1993).

[14] T. Yu and M. C. Lin, J. Am. Chem. Soc. **115**, 4371 (1993).

[15] J. J. Scherer, D. Voelkel, D. J. Rakestraw, J. B. P. C. Collier, R. J. Saykally, and A. O'Keefe, Chem. Phys. Lett. **245**, 303 (1995).

[16] G. Meijer, M. G. H. Boogaarts, R. T. Jongma, D. H. Parker, and A. M. Wodtke, Chem. Phys. Lett. **217**, 112 (1994).

[17] R. T. Jongma, M. G. H. Boogaarts, and G. Meijer, J. Mol. Spectrosc. **165**, 303 (1994).

[18] R. T. Jongma, M. G. H. Boogaarts, I. Holleman, and G. Meijer, Rev. Sci. Instrum. **66**, 2821 (1995).

[19] P. Zalicki and R. N. Zare, J. Chem. Phys. **102**, 2708 (1995).

[20] W. H. Press, B. F. Flannery, S. A. Teukolsky, and W. T. Vetterling, *Numerical Recipes in C: The Art of Scientific Computing* (Cambridge University Press, Cambridge, 1988).

[21] J. Cariou and P. Luc, *Atlas du Spectre d'Absorption de la Molecule de Tellure (Isotope 130)* (Laboratoire Aime-Cotton, CNRS II, 91405 Orsay, 1980).

[22] K. Yoshino, J. R. Esmond, J. E. Murray, W. H. Parkinson, A. P. Thorne, R. C. M. Learner, and G. Cox, J. Chem. Phys. **103**, 1243 (1995).

[23] Y. L. Huang and R. J. Gordon, J. Chem. Phys. **94**, 2640 (1990).

[24] R. N. Zare, A. L. Schmeltekopf, W. J. Harrop, and D. L. Albritton, J. Mol. Spectrosc. **46**, 37 (1973); a copy of the computer program LINFIT was provided by the authors.

[25] C. Amiot and J. Verges, Can. J. Phys. **59**, 1391 (1981).

[26] J. M. Hutson, J. Phys. B **14**, 851 (1981); a copy of the computer program CDIST was provided by the author.

[27] H. Partridge, C. W. Bauschlicher, S. R. Langhoff, and P. R. Taylor, J. Chem. Phys. **95**, 8292 (1991).

[28] R. W. Field and H. Lefebvre-Brion, Act. Phys. Hung. **35**, 51 (1974); see also H. Lefebvre-Brion and R. W. Field, *Perturbations in the Spectra of Diatomic Molecules* (Academic, Orlando, 1986), p. 104.

[29] R. Klotz and S. D. Peyerimhoff, Mol. Phys. **57**, 573 (1986).

[30] T. G. Slanger and P. C. Cosby, J. Phys. Chem. **92**, 267 (1988).

[31] G. Herzberg, Can. J. Phys. **30**, 185 (1952).

[32] V. Hasson and R. W. Nicholls, J. Phys. B **4**, 1778 (1971).

[33] B. R. Lewis and S. T. Gibson, Can. J. Phys. **68**, 231 (1990).

[34] M. W. P. Cann and R. W. Nicholls, Can. J. Phys. **69**, 1163 (1991).

[35] J. P. England, B. R. Lewis, and S. T. Gibson, J. Chem. Phys. (in press).

[36] R. P. Saxon and B. Liu, J. Chem. Phys. **67**, 5432 (1977).